Prediction of water resources in the Chao Phraya River Basin, Thailand

SUPATTANA WICHAKUL, YASUTO TACHIKAWA, MICHIHARU SHIIBA & KAZUAKI YOROZU

Dept. of Civil and Earth Resources Engineering, Kyoto University, Kyoto 615-8540, Japan
supattana@hywr.kuciv.kyoto-u.ac.jp

Abstract This study aimed to predict change in water resources in the Chao Phraya River Basin using outputs of the super-high-resolution general circulation model version MRI-AGCM3.2S for three different climate experiments: the present climate (1979–2008), near future climate (2015–2044), and future climate (2075–2104). In this study we used a regional distributed hydrologic model based on the concept of the variable infiltration capacity to generate runoff intensity in each computational grid. For flow routing, a kinematic wave model including effects of dam operation and inundation, was used. The C.2 gauging station at Nakhon Sawan was selected to monitor changes in the river discharge. The results showed water availability to considerably increase in the future climate experiment and drought risk to increase in the near future climate experiment. A statistical analysis of peak discharges was suggested for further study on evaluation of flood risk in the basin.

Key words runoff prediction; water resources projection; flow routing model; dam operation model; inundation model; Chao Phraya River Basin

INTRODUCTION

Climate change has an obvious impact on water resources. The magnitude and frequency of water related disasters, e.g. floods and droughts, are more likely to increase worldwide (Arora & Boer, 2001). For example, in the second half year of 2011 a devastating flood caused by continuous intense precipitation, occurred in the Chao Phraya River Basin (CPRB) in Thailand. The nation's economic system was severely disrupted, people lost their homes and lives were lost. From these situations it is realized that it is critical to assess the vulnerability of river systems and water-related disasters. There are some studies related to the impact of climate change in the CPRB. Hunukumbura & Tachikawa (2012) projected future river discharge to detect hotspots in river discharges in the CPRB using MRI-AGCM3.1s. Duong *et al*., (2013) used runoff data generated by MRI-AGCM3.2s to project a change in river discharge in the Indochina Peninsula region. As a distributed hydrological model is an important tool for achieving the study of future situations of water resources, Wichakul *et al*. (2013b) developed a regional distributed hydrological model including a dam operation model and inundation effects for the CPRB and tested the model performance with the 2011 flood and other historical extreme events.

This paper is focused on projecting the effect of climate change on the water resources situation of the CPRB, especially flow in the Chao Phraya River, by utilizing outputs of the latest 20 km spatial resolution general circulation model (MRI-AGCM3.2S) with the regional distributed hydrological model.

STUDY AREA AND INPUT DATA

The Chao Phraya River originates in the northern region of Thailand and flows from north to south. The total catchment area of the CPRB is 157 925 km^2. The annual precipitation is approx. 1400 mm. The upper part of the basin consists of four main tributaries: the Ping, Wang, Yom, and Nan rivers. The confluence of the Ping River and Nan River in Nakorn Sawan province is the beginning of the Chao Phraya River. There are two large storage dams, the Bhumibol Dam and the Sirikit Dam located in the Ping River basin and in the Nan River basin, respectively. Figure 1 shows the CPRB with a satellite image of inundated areas during the 2011 flood. To evaluate river discharge in the Chao Phraya River basin, the C.2 gauging station at Nakhon Sawan, located about 5 km downstream of the beginning of the river (15°40′N and 100°06′E), was selected as a monitoring station that represents the overall situation of the CPRB.

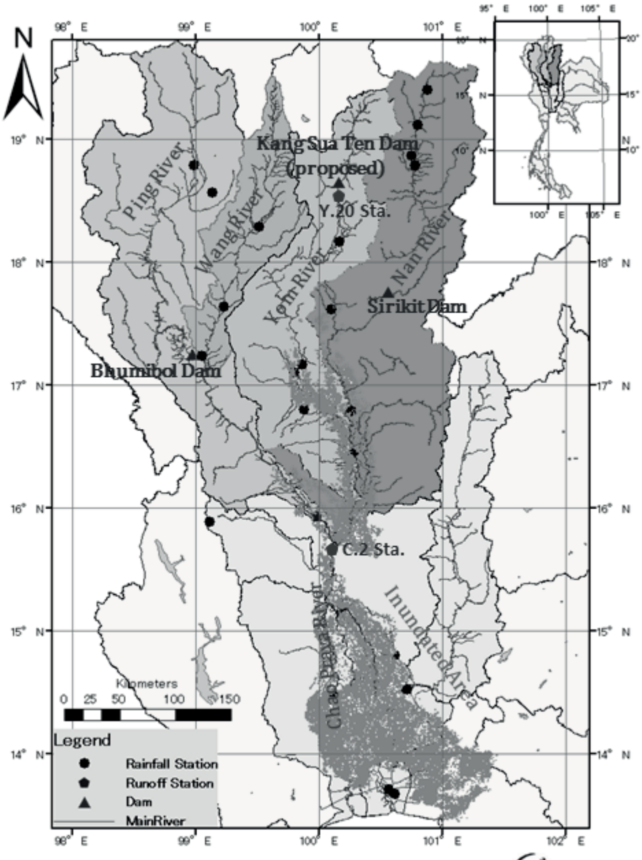

Source : Satellite image of inundated area by GISTDA

Fig. 1 Diagram of the Chao Phraya River Basin including the area inundated during the flood 2011.

In this study, we used rainfall and evapotranspiration data from gridded outputs of the super-high-resolution general circulation model, MRI-AGCM3.2S developed by the Meteorological Research Institute, Japan Meteorology Agency. The products of MRI-AGCM3.2S represented the present climate experiment (1979–2008), the near future climate experiment (2015–2044), and the future climate experiment (2075–2104), which were simulated under a global warming A1B emission scenario (Mizuta *et al*., 2012). The GCM output variables, i.e. PRCSL (rainfall reaching to soil layer), EVPSL (evaporation from bare soil), and TRSNL (transpiration from root zone soil), were used without bias-correction as input rainfall and evapotranspiration to a distributed hydrological model for runoff generation. The input data to the distributed hydrological model represented 1120 (28 columns and 40 rows) grid cells covering the CPRB.

DISTRIBUTED HYDROLOGICAL MODEL

In this study, to deal with the GCM output for water resources projection, a regional distributed hydrological model including dam operation and inundation effects was used to generate the river discharge. The model was developed and evaluated using observed time series discharge of the 2011 flood and other historical extreme events in the CPRB. The overall model performance achieved a Nash-Sutcliffe model efficiency coefficient of 0.91 and a squared correlation coefficient of 0.94 for the calibrated period at C.2 station (Wichakul *et al*., 2013a,b). Development details for each part of the model are explained in the following sections.

Rainfall–runoff model: simplified Xianjiang (SXAJ) model

The water budget at each computational grid cell was simulated by the SXAJ model. Rainfall intensity r and evapotranspiration intensity e (mm.h^{-1}) were transformed to total runoff intensity Q

by a function of the SXAJ model. The relationship between runoff and infiltration distribution as a function of grid wetness and infiltration capacity is illustrated in Fig. 2.

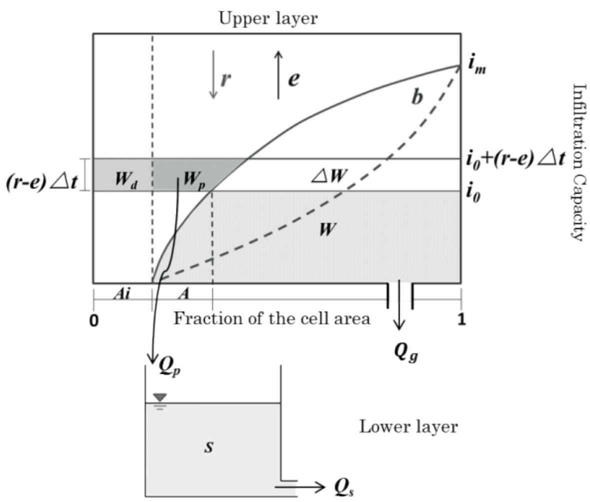

Fig. 2 Function of the SXAJ model based on the concept of variable infiltration capacity.

Direct runoff intensity Q_d and subsurface runoff intensity Q_s were combined to give total runoff. Variable infiltration capacity i over an area is expressed as follows:

$$i = \begin{cases} 0 & if \quad 0 \le A \le A_i \\ i_m \left[1 - \left(1 - \dfrac{A - A_i}{1 - A_i} \right)^{1/b} \right] & if \quad A_i \le A \le 1 \end{cases} \tag{1}$$

where i_m represents the maximum infiltration capacity, A is the fraction of cell area for infiltration capacity, and takes values between 0 and 1, A_i is the portion of direct runoff generation area in the cell, and b is an empirical parameter showing the storage water capacity curve (b>1 represented by the dashed curve). From equation (1), by integration, the maximum tension water storage of the cell W_m and current soil moisture W can be calculated and varied from zero to a maximum point. The depth of direct runoff W_d was directly generated form A_i area. The surface runoff depth W_p (dark shaded area) was calculated using the relationship of the integral function and the area above the infiltration capacity curve depended on the amount of rainfall and evapotranspiration and current infiltration capacity i_0.

Surface runoff component Q_p (in mm/h) infiltrates to result in the model's subsurface runoff (base flow) component as illustrated in Fig. 2 (lower layer). The model's subsurface runoff component was approximated by the relationship of a nonlinear reservoir and continuity equation. As shown in Fig. 2, the effect of the groundwater component was included in the upper layer of the model. Consequently, the soil water storage contributes to groundwater Q_g expressed by the function of a nonlinear reservoir relationship. The best combination for the model parameters was estimated using 2011 observed discharge data at the Bhumibol and Sirikit dams and the C.2 station. Observed data for 1995, 2008 and 2010 at these three locations was also compared to simulated discharge to verify model parameters (Wichakul *et al*., 2013a). The model resolution is equivalent to the resolution of the GCM output and a 1-h time step of calculation.

Flow routing Model: 1K-FRM

1K-FRM (Tachikawa *et al*., 2011) is a 1 km resolution flow routing model for channel routing in the upper part of the CPRB in this study. The total runoff of each computational grid was routed downstream based on a one-dimensional kinematic wave equation. To project future situations of water resources in the CPRB, dam operation and inundation models were developed and embedded in the 1K-FRM (Wichakul *et al*., 2013b). The model represents 288 000 (480 columns and 600 rows) computational grid cells and used a 10-min time step of calculation. Topographic data used in the 1K-FRM were the 30-arc-second DEM and flow direction stored in HydroSHED (USGS, 2001). Details of the development of these two models are explained in the sections that follow.

Dam operation model

Due to the location of the Bhumibol and Sirikit dams (as illustrated in Fig. 1), Chao Phraya River water flow is significantly influenced by the operation of these storage dams. It was therefore, considered that a dam operation model was necessary in the simulation. In this paper, to model the dam operation situations in future, we considered min/max storage instead of a rule based curve on the assumption that water released in the dry season (January–April) was determined by a minimum reservoir storage and downstream requirement, and in the wet season (May–December) was determined by a min/max reservoir storage and spillway capacity.

Inundation model

The concept of the diffusive tank model was adopted (Moussa & Bocquillon, 2009) by considering the drainage discrepancy between the main channel and floodplain ponds for the purpose of including the inundation effect. The original kinematic wave equation was modified as follows:

$$\frac{\partial A}{\partial t}+\frac{\partial Q}{\partial x}=q(t)-q_{li}(t) \tag{2}$$

where $q(t)$ is lateral inflow per unit length of channel unit given as runoff generated by the SXAJ model and q_{li} is exchange lateral overbank flow per unit width solved by this inundation model. The exchange lateral overbank flow between the channel and floodplain area was modelled using a broad crested weir equation for a clear overflow weir (river bank). To model the recession flow back process to the channel, we identified lateral flow q_{li} by modifying a concept of Darcy's law.

ASSESSMENT ON CLIMATE CHANGE

Variability and trends of GCM outputs

By analysing rainfall and evapotranspiration data derived from GCM outputs, PRCSL (rainfall on the land surface), EVPSL (evaporation from bare soil) and TRSNL (transpiration) for three different climate experiments, Table 1 presents mean annual rainfall and evapotranspiration presented at the C.2 gauging station grid located at the middle of the entire CPRB (Fig. 1). Mean annual rainfall slightly decreased in the near future climate experiment and significantly increased in the future climate experiment. Annual evapotranspiration also tends to be constant in the near future climate experiment. That change varied by less than 1% from the present climate annual evapotranspiration. In contrast, in the future climate experiment, both rainfall and evapotranspiration shows a rising trend of approximately 5% and 4% from the present climate, respectively. Figure 3(a) shows that fluctuation of mean annual rainfall during the future climate experiment and the difference of the lowest and highest values. Mean annual evapotranspiration shows similar fluctuations for all three climate experiments, as presented in Fig. 3(b).

Most of the northern part of the CPRB is covered by forest and mountainous areas, so the total amount of mean annual rainfall and evapotranspiration of this area is higher than the central and lower part of the basin. In terms of spatial distribution of trend the mean annual rainfall change throughout the basin has a similar rate and pattern to the C.2 grid for the near future climate experiment. The trend of mean annual rainfall has a different rate and pattern for the future climate experiment by decreasing values around the edge of the basin. The mean annual evapotranspiration trend keeps a similar rate and pattern of change throughout the basin for both near future and future climate experiments. These changes of rainfall and evapotranspiration show that the water availability trends (approximated runoff) reduced by about 7% in the near future climate and increased by about 7% in the future climate.

Table 1 Mean annual rainfall and evapotranspiration.

At C.2 gauging station grid	Present (SPA)	Near Future (SNA)	Future (SFA)
(1) Rainfall on the land surface in mm	1192	1169	1247
(2) Evapotranspiration in mm	957	951	996
(3) Approximated runoff in mm (1)–(2)	235	218	251

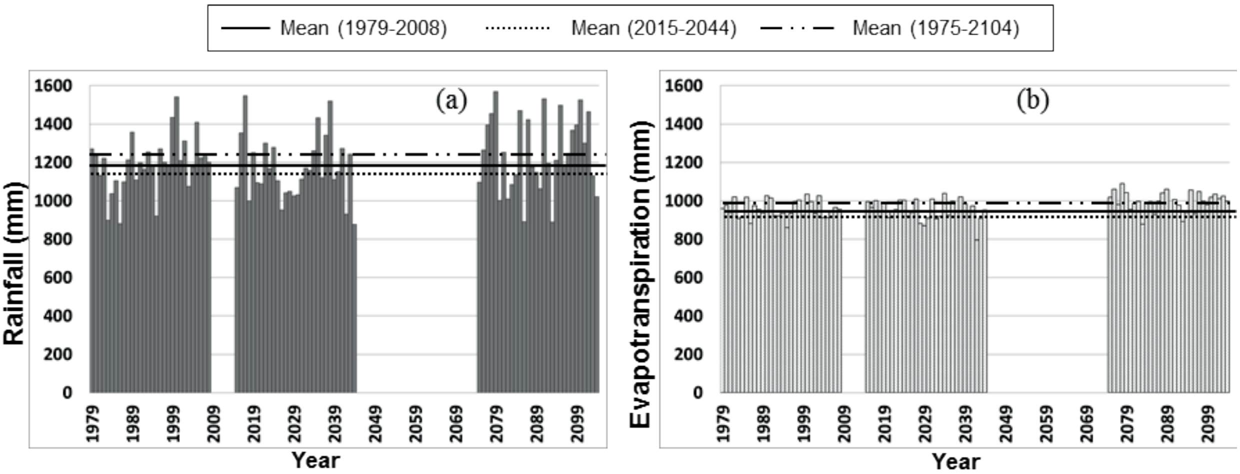

Fig. 3 (a) Annual rainfall and (b) evapotranspiration data in the C.2 station grid.

Change in river discharge

Details of the change in river discharge by analysing simulated discharge from the distributed hydrological model is discussed in this section. As shown in Fig. 4(a), observed daily discharge data were collected and compared with simulated discharge for the present climate experiment at the C.2 station. Due to no bias correction, simulated discharge generally tended to overestimate during wet seasons. But during the low flow period simulated discharge was close to the observed discharge. Therefore, it is reasonable and realistic to evaluate drought risk in this study. However, a tendency for change in overall water availability in the CPYB was also foreseen.

Figure 4(b) shows the comparison of mean monthly discharge at the monitoring station for three climate experiments. Mean monthly discharge of most of the months, excepting May, shows considerable increases for the future climate. For the near future, the mean monthly discharge in May and August is lower than the present climate experiment. According to the flow routing model including dam operation, discharge during the dry season (January–April) was under regulated by the dam model. It means that most of the river discharge was released from storage water in the dams in the dry season. However, it was difficult to get a clear change on river discharge by this comparison of mean monthly discharge.

Flow duration curves show the probability of exceedence of flow magnitude and help to characterize the response of the river to a changing climate. Figure 5(a) shows mean annual flow duration curves with standard deviations for the three climate experiments. For the future climate, a considerable increase in all discharge rates (both high and low flow section) is consistent with the rate of rainfall increases rather than evapotranspiration. For the near future climate, a slight increase in mean discharge rates at the middle flow section and a decrease at the low flow section was detected. To enlarge the low flow section, Fig. 5(b), therefore, compares the flow duration curves constructed based on daily discharge of a period-of-record of each climate experiment at the low flow section. Hence, it is clear that the low flow values tend to decrease significantly in the near future experiment and result in increased drought risk in the CPRB.

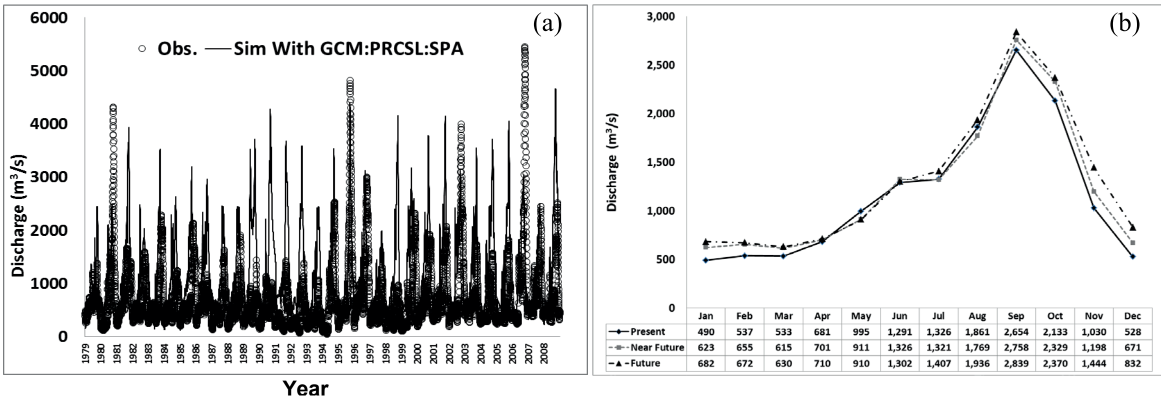

Fig. 4 (a) Comparison of observed and simulated discharge with GCM outputs for present climate at the C.2 station. (b) Mean monthly discharge at the C.2 station for the present, near future and future climate experiments.

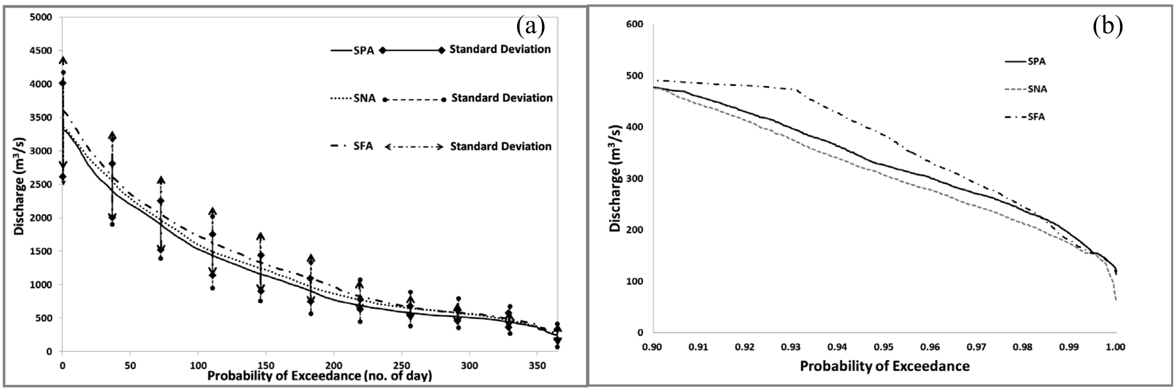

Fig. 5 (a) Mean annual flow duration curves with standard deviation of the present climate (SPA), near future climate (SNA), and future climate (SFA) experiments. (b) Low flow section of the flow duration curves constructed based on daily discharge of a period-of-record of each climate experiment.

CONCLUSION

In this study, a regional distributed hydrological model, including the effect of dam operation and inundation and outputs of the MRI-AGCM3.2S, PRCSL, TRNSL and EVPSL, were applied to the CPRB for projected river discharge in the present climate (1979–2008), the near climate future (2015–2044) and the future climate (2075–2104) experiments. Changes of rainfall and evapotranspiration, which were derived for the GCM outputs, showed that the water availability trends reduced in the near future climate experiment and increased in the future climate experiment. This result was comparable with the result from our simulation by the model. Broad trends of projected discharge showed that water availabilities in the CPRB increase all year round, both in the wet and dry seasons in the future climate experiment. For the near future climate, annual water budget slightly increases, but during dry season trends of projected discharge reduced considerably.

According to our study results, reduction of water availability led to an increase in drought risk in the near future climate. By using the application of the dam operation model, an adaptive measure for managing dam operation rules to deal with the risk of drought is recommended for further study. It was difficult to achieve reliable estimates of peak discharges under climate change conditions at this stage. Therefore, a statistical method based on the relationship between observed and simulated peak discharges was suggested to be conducted for further study on the projection of water resources of the CPRB. From the information of change of drought risk and flood risk, proposed dam operation rules might be helpful for sustainable planning of water resources management of the basin.

REFERENCES

Arora, V. K. & Boer, G. J. (2001) Effect of simulated climate change on the hydology of major river basins. *J. Geophys. Res.* 106(D4), 3335–3348.

Duong, D. T., Tachikawa, Y., Shiiba, M. & Yorozu, K. (2013) River discharge projection in Indochina peninsula under a changing climate using the MRI-AGCM3.2S dataset. *J. Japan Society of Civil Engng B1 (Hydraulic Engng)* 69(4), 37–42.

Hunukumbura, P. B. & Tachikawa, Y. (2012) River Discharge Projection under Climate Change in the Chao Phraya River Basin. *J. Meteorol. Soc. Japan* 90(A), 137–150.

Mizuta, R., Yoshimura, H., Murakami, H., Matsueda, M., Endo, H., Ose, T., Kamiguchi, K., Hosaka, M., Sugi, M., Yukimoto, S., Kusunoki, S. & Kitoh, A. (2012) Climate simulation using MRI-AGCM3.2 with 20-km Grid. *J. Meteorol. Soc. Japan* 90(A), 233–258.

Moussa, R. & Bocquillon, C. (2009) On the use of the diffusive wave for modelling extreme flood events with overbank flow in the floodplain. *J. Hydrol.* 374, 116–135.

Tachikawa, Y., Takino, S., Fujioka, Y., Yorozu, K., Kim, S. & Shiiba, M. (2011) Projection of river discharge of Japanese river basins under a climate change scenario (in Japanese). *J. Japan Society of Civil Engng B1 (Hydraulic Engng)* 67(1), 1–15.

USGS (2001) HydroSHEDS. http://hydrosheds.cr.usgs.gov/

Wichakul, S., Tachikawa, Y., Shiiba, M. & Yorozu, K. (2013a) Developing a regional distributed hydrological model for water resources assessment and it application to the Chao Phraya River Basin. *J. Japan Society of Civil Engng B1 (Hydraulic Engng)* 69(4), 43–48.

Wichakul, S., Tachikawa, Y., Shiiba, M. & Yorozu, K. (2013b) Development of a flow routing model including inundation effect for the extreme flood in the Chao Phraya River Basin, Thailand 2011. *J. Disaster Research* 8(3), 415–423.